A reaction norm for flowering time plasticity reveals physiological footprints of maize adaptation

Justine Drouault[1], Carine Palaffre[2], Emilie J. Millet[1], Jonas Rodriguez[1], Pierre Martre[1], Kristian Johnson[1], Boris Parent[1], Claude Welcker[1], Randall J. Wisser[1,3*]

[1]LEPSE, University of Montpellier, INRAE, Institut Agro Montpellier, Montpellier, FR

[2]Experimental Unit of Maize, INRAE, 40390 Saint Martin De Hinx, FR

[3]Department of Plant and Soil Sciences, University of Delaware, Newark, Delaware, USA

***Correspondence:** Randall J. Wisser, randall.wisser@inrae.fr

ORCIDs: EJM: 0000-0002-2913-4892; JR: 0000-0001-8693-1022; PM: 0000-0002-7419-6558; CW: 0000-0002-8275-1259; RJW: 0000-0003-1075-0115

Current address:

Emilie J. Millet: INRAE, UR1052 GAFL, 84143 Montfavet, France

Jonas Rodriguez: Syngenta Seeds, P.O Box 18300, Greensboro, North Carolina, USA

keywords: Adaptation, GxE, Envirotyping, Flowering time, Maize

Running title: Flowering time plasticity in maize

Date of submission: April 10, 2025

Number of tables and figures

Tables: 2
Figures: 5

Supplementary data

Tables: 1
Figures: 2
Files: 6

Abstract

Understanding how plant phenotypes are shaped by their environments is crucial for addressing questions about crop adaptation to new environments. This study focused on analyzing the genetic variability underlying genotype-by-environment interactions and adaptation for flowering time in maize. We present a physiological reaction norm for flowering time plasticity (PRN-FTP), modeled from multi-environment trial networks and decomposed into its physiological components. We show how genotype-specific differences in developmental responses to temperature fluctuations condition differences in photoperiod perceived among genotypes. This occurs not only across but also within common environments, as the perception of photoperiod is altered by variation in rates of development and durations for becoming sensitized to photoperiod. Using a new metric for envirotyping sensed photoperiods for maize, it was found that, at high latitudes, different genotypes in the same environment can experience up to hours-long differences in photoperiod. This emphasizes the importance of considering genotype-specific differences in the experienced environment when investigating plasticity. Modeling the PRN-FTP for globally representative breeding material showed that tropical and temperate germplasm occupy distinct territories of the trait space for PRN-FTP parameters. Placed in the historical context of maize, our findings suggest that the geographical spread and breeding of maize was mediated by a specific modality of ecophysiological adaptation of flowering time. Our study has implications for understanding crop adaptation and for future crop improvement efforts.

Article Summary

Maize adjusts its flowering time across environments using genetic pathways tuned to cues like temperature and day length. This study models how different varieties perceive and respond to these factors, revealing that genotypes can perceive the same environment in distinct ways. By disentangling the ecophysiological basis of genotype-environment interactions, the research explores maize diversity and highlights how adaptation and breeding have shaped distinct strategies for flowering time regulation in tropical and temperate varieties.

Introduction

Plants exhibit vast phenotypic diversity, the principal axis for adaptation and evolution. The classic formalism $P = G + E + G \times E$ describes how phenotypes are determined by combinations of genetic (G) and environmental (E) effects. Environmental effects result from varying external conditions that lead to distinct phenotypic outcomes for the *same* genotype, a phenomena known as plasticity (Bradshaw, 1965). As 21st-century climate markedly shifts the environmental dimension to new frontiers, it is an important and opportune time to investigate plasticity (E) and genetic variation in plastic responses ($G \times E$). For crop improvement, harnessing plastic responses to shifts in climate conditions can facilitate the adaptation of crops into new territories or to alternative cropping systems (Rising and Devineni, 2020; Sloat *et al.*, 2020; Zabel *et al.*, 2021). Thus, approaches for modeling $G \times E$ that are rooted in the understanding of plasticity represent a promising direction for agricultural research (e.g., Millet *et al.*, 2019; Cooper *et al.*, 2020; van Voorn *et al.*, 2023).

The functional relationship that defines a pattern of plasticity across an environmental gradient is known as a reaction norm, with parameters that quantify the direction and magnitude of phenotypic change (Roof, 1997). The reaction norm provides a foundation for modeling phenotypic responses to the environment. However, separate disciplines have conceived of reaction norms in different ways. A common approach in quantitative genetics uses the *Finlay–Wilkinson* statistical model applied to multi-environment trials (METs) (Finlay and Wilkinson, 1963), in which the phenotypic values of individual genotypes are regressed on an index defined by the mean values of all genotypes per environment. In this framework, phenotypes are typically for final characteristics measured at the whole-plant scale that are targets for selection, such as flowering time, plant height, or yield. This method has provided a convenient generalization for modeling reaction norms from METs where large collections of genotypes can be simultaneously tested across different environments, enabling a widescale analysis of $G \times E$ (Jarquín *et al.*, 2014; Kusmec *et al.*, 2017; Guo *et al.*, 2023). Clearly, however, the environment is abstractly defined and confounded with latent environmental effects where mechanisms underlying $G \times E$ become elusive, resulting in a lack of biological interpretability. In contrast, focused on phenotyping of finer-scale traits in controlled settings, ecophysiologists have characterized norms of reaction for physiological responses to specific environment variables, such as the non-linear response of growth and development to temperature (Parent *et al.*, 2010; Parent and Tardieu, 2012). Embedding formalisms for such reaction norms in crop growth models allows an upscaling to the phenotypes for final characteristics. This is modeled as a function of genotype-specific parameters and environmental conditions, with outcomes emerging from physiological mechanisms that dynamically regulate plant development in response to fluctuating conditions across time (Muller and Martre, 2019). This approach provides biological perspective, but studying broad diversity of $G \times E$ is challenged by experimental constraints to measuring the parameters of physiological reaction norms. In our study, we hypothesized that parameterizing a physiological reaction norm from MET data would allow us to analyze the diversity of flowering time plasticity in maize (*Zea mays* subsp. *mays*) and provide unique insights into maize adaptation.

Physiological responses to multiple environmental factors modulate development which affects flowering time, particularly temperature and photoperiod (Simpson and Dean, 2002; Colasanti and Coneva, 2009; Blümel *et al.*, 2015; Lee *et al.*, 2021). The influence of temperature results in a speeding or slowing of development, while, for photoperiod sensitive genotypes, the influence of photoperiod results in the suppression of reproductive transition and a delay in flowering time (this occurs under long daylengths for short-day species and short daylengths for long-day species). The response to temperature occurs throughout a plant's life cycle, while the response to photoperiod is growth-stage specific. This is a crucial distinction for the work presented here. In maize, a facultative short-day (SD)

species, the stage at which plants become sensitized to photoperiod is not directly observable, but based on photoperiod-swap experiments has been found to occur immediately before tassel initiation (reproductive transition) if plants are grown specifically under SD conditions (Kiniry *et al.*, 1983*b*; Bassiri *et al.*, 1992). In SD conditions, tassel initiation is not repressed by photoperiod and temperature is the primary driver of development time and determinant for when a genotype reaches the sensitized stage. Above a critical photoperiod, under long-day (LD) conditions, tassel initiation in photoperiod sensitive genotypes is delayed beyond the timing at which they reach their sensitized stage, with a time delay that depends on genotypic variation in the degree of photoperiod sensitivity in addition to temperature fluctuations during the period of delay. Thus, as physiological responses to temperature fluctuations across the development cycle interact with genotypic variation in rates of plant development and durations of the reproductive transition, different genotypes can reach the sensitized stage on different days, and therefore perceive different photoperiods, even within the same environment. For photoperiod sensitive genotypes, the magnitude of response to photoperiod is an additional source of plasticity that varies genetically, culminating in the formation of $G \times E$ interactions in flowering time across environments. We introduce these first-principles expectations for $G \times E$ interactions in flowering time, but we are not aware of studies that have considered this in the construction of reaction norms from MET data.

The timing of reproductive transition (and consequently flowering) is controlled by a genetic regulatory network (GRN) that integrates both the exogenous and endogenous signals (Song *et al.*, 2015). A reference topology of this GRN in maize consists of multiple pathways including the circadian clock, photoperiod, autonomous, aging, and gibberellic acid pathways (Dong *et al.*, 2012). However, the complete topology and context-dependent expression of the GRN is far from being fully understood (Minow *et al.*, 2018; Stephenson *et al.*, 2019). A key distinction exists in the way the GRN functions between LD and SD environments, with daylength-dependent and daylength-independent responses for photoperiod sensitive and insensitive genotypes. For example, the circadian clock pathway plays a central role in the transduction of signals to the other pathways, with a direct link between external light conditions and the photoperiod pathway (in both LD plants like Arabidopsis – Sawa *et al.*, 2007; Sawa and Kay, 2011; and SD plants like maize - Bendix *et al.*, 2013). Under LD conditions, transduction of light perception by the circadian clock to the photoperiod pathway represses production of the *FT*-derived florigen signal for reproductive transition in photoperiod sensitive genotypes of maize—flowering time is delayed (Meng *et al.*, 2011). In contrast, the mechanism controlling floral transition is configured differently in insensitive genotypes of maize, with recent research implicating separate clock components that interact with the autonomous pathway (Minow *et al.*, 2018). Less is known about the determination of critical thresholds for photoperiod sensitivity. A gating mechanism involving the circadian clock and photoperiod pathways has been described in rice (a facultative SD species like maize; Itoh *et al.*, 2010; Nemoto *et al.*, 2016), with additional findings suggesting a conditional link involving the autonomous pathway described in maize (Matsubara *et al.*, 2008; Park *et al.*, 2008).While molecular genetic studies continue to elucidate the intricate dynamics of cross-talk and signal transduction by the GRN, a challenge is to relate this to functional diversity at the whole plant level. Thus, new approaches to characterizing the wider scale variation in ecophysiological plasticity for flowering time are needed.

This study focused on the modeling and analysis of a physiological reaction norm for flowering time plasticity (PRN-FTP) that integrates genotype-specific sensing and responses in growth and development to fluctuating temperatures and photoperiods, ultimately resulting in $G \times E$ for flowering time. Building on previous work (Kiniry *et al.*, 1983*a,b*; Choquette *et al.*, 2023), the PRN-FTP was formulated as a bilinear, threshold-dependent function that relates thermal time from crop emergence to flowering with a novel envirotyping index for the daylength sensed (DL^{s}) by individual genotypes

in each environment. We envirotyped DL^s across field environments in the Northern Hemisphere to understand how photoperiod perception varies among genotypes both within and across environments, and whether genotype-specific values for DL^s should be used for modeling the PRN-FTP. We further demonstrate how analyzing the PRN-FTP as a bilinear function allows the decoupling of different components of flowering time variation: (i) flowering time *per se*; (ii) critical photoperiod; and (iii) photoperiod sensitivity; with genotype-specific parameter values estimated from MET data.

Finally, PRN-FTP parameters may be used to understand how flowering time plasticity varies among population groups or mediates adaptation to novel environments, and how this in turn alters flowering time plasticity for the future. Historical varieties of maize that spread from their tropical origins into temperate zones required adaptations to cooler climates with longer photoperiods, with studies implicating the central role of flowering time (Tenaillon and Charcosset, 2011). For instance, several flowering time genes in the GRN for flowering time have been linked to the post-domestication spread of maize (e.g., *Vgt1* – Ducrocq *et al.*, 2008; *ZmCCT10* – Hung *et al.*, 2012; Yang *et al.*, 2013; *ZCN8* - Guo *et al.*, 2018; *ZmELF3.1* – Zhao *et al.*, 2023). Here, we show that the trait space relating variation in the PRN-FTP parameters flowering time *per se* and photoperiod sensitivity putatively reflects how adaptation and selection history has shaped differences in flowering time plasticity between breeding pools of modern maize.

Materials and Methods

A general guide to the study design and use of datasets 2-4 is presented in Fig. 1.

Datasets

Summarized in Table S1, datasets ("D") from multiple projects and experiments on maize were assembled to: (D1) select a temperature response function for thermal time estimation; (D2) develop a predictor function for DL^s; (D3) envirotype DL^s for diverse genotypes in fields across the Northern Hemisphere; (D4) demonstrate methods for modeling a physiological reaction norm for flowering time plasticity (PRN-FTP); and (D5) compare the trait space of parameters estimated from the PRN-FTP in a diversity panel constituting separate breeding pools of maize. A brief description of the datasets used for these five objectives are presented first, followed by methods and other details in subsequent sections. The current study focused on days to anthesis (male flowering) as the final characteristic.

(D1) This dataset contains 24 hybrid genotypes measured for days to anthesis in 25 to 26 field experiments, spanning latitudes from 30.5371 °N to 44.2089 °N (File S1). For each environment, the sowing date, field coordinates, and best linear unbiased estimates (BLUEs) for calendar days from sowing to anthesis were obtained from McFarland *et al*., 2020 and Rogers *et al*., 2021.

(D2) This dataset contains a collection of 284 inbred genotypes (panel A) with trait data combined from two experiments. Emergence time and phyllochron were measured under well-watered conditions in a greenhouse phenotyping platform at the LEPSE of INRAE (PhenoArch, Montpellier, FR; Cabrera-Bosquet *et al.*, 2016). Final leaf number was measured under well-watered conditions in a field environment in Puerto Vallarta, MX. Both experiments were performed under SD conditions, where daylengths throughout the growth cycle never exceeded 12.5 h. Further details for these experiments and the estimation of genotypic effects can be found in Supplemental Information (Methods S2).

(D3) This dataset contains the geographical coordinates and planting dates for 671 field environments across the Northern Hemisphere (latitudinal range of 13.7578 °N to 54.2900 °N) assembled from previous and new projects (File S3).

(D4) This dataset contains a collection of seven temperate inbred genotypes (B37, B73, M37W, Mo17, Oh43, LH123Ht, and 2369) and seven tropical inbred genotypes (CML10, CML258, CML277, CML341, CML373, Tzi8, and Tzi9) measured for days to anthesis in 37 field experiments (File S4). Assembled from previous and new projects, it represents a multi-environment trial (MET) dataset designed to maximize the presence of these 14 genotypes, which were also included in dataset D2. However, their representation across environments was uneven, with temperate genotypes tested in 15 to 22 environments and tropical genotypes in 18 to 37 environments.

(D5) This dataset contains a collection of 109 temperate, 66 tropical, and 61 admixed inbred genotypes, representing separate breeding pools (panel B; Liu *et al.*, (2003); Flint-Garcia *et al.*, (2005)), measured for days to anthesis across an MET with a maximum of 19 field experiments (File S5). It was assembled from previous projects with an imbalanced representation of photoperiod conditions, including a maximum of three short-day (SD) environments (maximum photoperiod <12.4 h) and 16 long-day (LD) environments (minimum photoperiod >14.5 h), spanning latitudes from 18.00 °N to 42.76 °N.

Environmental data

For field environments considered in this study, temperature data were acquired from ground and satellite data sources for a common reference point of 2 m height. Ground data were obtained mostly from weather stations at a given field location. In two cases, ground data from a nearby airport within 5 km of the experimental field site was obtained from Weather Underground (https://www.wunderground.com/). Satellite data (weather variable 'T2M'; spatial resolution of ½° latitude x ⅝° longitude) was acquired from the R package *nasapower* (Sparks, 2018) using the latitude and longitude coordinates for each field location.

The photoperiod based on civil twilight at a given location for a given day of the year was acquired from the R package *TrenchR* (Buckley *et al.*, 2023). This uses the CBM daylength model described by Forsythe *et al.* (1995).

Comparison of temperature response functions

Throughout this study, calendar days were converted into thermal time to account for growth and development variations caused by temperature differences across field environments. We evaluated three temperature response functions for calculating thermal time using Dataset D1 (Methods S1, Eq. S1-S3). This comparison was based on the assumption that temperature-driven growth and development primarily determine the time to flowering in photoperiod-insensitive genotypes. Under this assumption, temperature differences alone should explain most of the variation in days to anthesis across environments. The function that produces the most consistent thermal time to anthesis values for a given genotype across environments would, therefore, be considered the best. Dataset D1 was used for this assessment since it consisted of temperate-adapted maize hybrids (generally known to be photoperiod insensitive) tested across many independent field environments.

For each of the 24 hybrids, BLUEs for days to anthesis from each field experiment were converted into thermal time using each function. Then, the normalized root mean square error (NRMSE, normalized by the difference between maximum and minimum values) of function-specific thermal times was computed for each genotype. The results were compared to identify the function that minimized the

NRMSEs overall. For the purpose of comparing different models for thermal time estimation with the same dataset, we assumed the influence of any latent variables on growth and development could be ignored.

Definition of a physiological reaction norm for flowering time

The PRN-FTP was reformulated from a previous model by Kiniry *et al.* (1983*a*) that described the relationship between photoperiod (x-axis) and thermal time from crop emergence to tassel initiation ($T_{\mathrm{t}}^{\mathrm{em-TI}}$) based on temporal dissections of shoot apical meristems (y-axis). Kiniry *et al.* (1983*a*) used growth chambers in which constant levels of photoperiod were applied throughout the plant's growth cycle, so DL^{s} had a known value in each treatment. However, in field environments photoperiods are not constant (DL^{s} depends on the day of year within a given environment when a plant become sensitized to photoperiod) and estimating tassel initiation from dissections of meristems is not practical at large scale (rather, in METs, days to flowering are routinely recorded). Besides, as mentioned above, even direct observation of tassel initiation does not correspond to the timing when photoperiod sensitive genotypes become sensitized to photoperiod in LD environments. Therefore, we devised an approach for predicting this unobservable stage of photoperiod sensitization, such that DL^{s} could be determined for a given genotype in a given environment. Thus, adapted for METs that cover SD and LD environments, this study defined the PRN-FTP as the relationship between a new proxy measure for DL^{s} (x-axis) and thermal time from crop emergence to anthesis ($T_{\mathrm{t}}^{\mathrm{em-ant}}$; y-axis).

Procedure for DL^{s} estimation. There are two main steps used for determining DL^{s}. First, the $T_{\mathrm{t}}^{\mathrm{em-TI}}$ is estimated for genotypes grown under SD conditions in which a photoperiod response is not triggered. In this study, an ecophysiological formalism was used to predict $T_{\mathrm{t}}^{\mathrm{em-TI}}$ (Eq. 1) from experimental data. This is expected to closely approximate the amount of thermal time it takes for a given genotype to become sensitized to photoperiod, which has been referred to as the basic vegetative phase (BVP; Kiniry *et al.*, 1983*b*). Second, the calendar day on which the total thermal time for the BVP is reached is determined using temperature records for a given environment. The daylength for that specific day is then obtained for DL^{s}. As applied in this study, the two steps of this procedure are as follows:

Step 1: An ecophysiological formalism (Eq. 1) was used to estimate BVP for the 284 genotypes in panel A that were phenotyped in SD experiments (Dataset D2; Methods S2). Therefore, even though the panel included photoperiod sensitive genotypes, their photoperiod responses were not triggered, such that estimates of $T_{\mathrm{t}}^{\mathrm{em-TI}}$ correspond to the BVP. Considering that tassel initiation occurs on the day when the last leaf primordium is formed (Lejeune and Bernier, 1996) and that rates of leaf primordia formation and leaf tip appearance are proportional (Padilla and Otegui, 2005), $T_{\mathrm{t}}^{\mathrm{em-TI}}$ can be calculated as:

$$T_{\mathrm{t}_i}^{\mathrm{em-TI}} = \frac{P_{\mathrm{tip}_i}}{\alpha_{\mathrm{phyll/plast}}}\left(L_{\mathrm{F}_i} - L_{\mathrm{pri}}^{\mathrm{em}}\right) \qquad \text{(Eq. 1)}$$

where, $T_{\mathrm{t}_i}^{\mathrm{em-TI}}$ (°Cd) is the cumulative thermal time from crop emergence to tassel initiation of the ith genotype, P_{tip_i} (leaf °Cd^{-1}) is the phyllochron of the ith genotype (i.e., the thermal time between the appearance of two successive leaf tips), L_{F_i} (leaf) is the final leaf number of the ith genotype, $\alpha_{\mathrm{plast/phyll}}$ (dimensionless) is a constant ratio of phyllochron to plastochron (i.e., the thermal time between the formation of two successive leaf primordia), and $L_{\mathrm{pri}}^{\mathrm{em}}$ (primordium) is a constant number of primordia formed at crop emergence. Genotype-specific values for P_{tip_i} and L_{F_i} were estimated for panel A (Dataset D2; Methods S2). For maize, $\alpha_{\mathrm{plast/phyll}}$ may range from 1.58 to 1.85 (Kiniry, 1991; Lejeune and Bernier, 1996; Padilla and Otegui, 2005; Andrieu *et al.*, 2006). In this study, we set it at

the average value reported in the literature (1.73). There are four to five leaf primordia in the embryo of maize seeds (Bonnett, 1954; Padilla and Otegui, 2005), and between germination and crop emergence about two other leaf primordia are formed (Padilla and Otegui, 2005). Thus, here, $L_{\mathrm{pri}}^{\mathrm{em}}$ was set equal to 5.5 primordia.

Step 2: Using $T_{\mathrm{t}}^{\mathrm{em-TI}}$ for the BVP of a given genotype, along with emergence date and temperature records from a given environment, the calendar day on which the genotype becomes sensitized to photoperiod was predicted. When observed emergence dates were unavailable, a thermal time of 76 °Cd was assumed for the period from sowing to emergence. This was estimated from observed data for 15 environments within Dataset D4 (sourced from the Maize ATLAS project; see Table S1), calculated using the temperature response function Eq. S2.

Thermal time from crop emergence to anthesis (y-axis of the PRN-FTP).

For each genotype in each environment, $T_{\mathrm{t}}^{\mathrm{em-ant}}$ was calculated as the cumulative thermal time between the dates of emergence date (observed or predicted) and anthesis (determined from BLUEs of days to anthesis).

Envirotyping sensed photoperiod

Dataset D3 was used to computationally envirotype DL^{s} across 671 environments in the Northern Hemisphere. In each environment, DL^{s} was envirotyped for three maturity levels defined by the lower (5th; early maturity), median (50th), and upper (95th; late maturity) percentiles of the BVP distribution estimated for panel A (Dataset D2; Table 1). The difference in DL^{s} between maturity levels was calculated to assess how genotypes with different BVPs may vary in the photoperiod they perceive within a given environment. Knowing that daily changes in photoperiod increase with latitude, the per-environment differences in DL^{s} were compared to rates of photoperiodic change. The rate of photoperiodic change within each environment was calculated from photoperiods between the days immediately before and immediately after DL^{s} for the 50th-percentile maturity level.

When modeling the PRN-FTP for each genotype from MET data, $T_{\mathrm{t}}^{\mathrm{em-ant}}$ (response variable) values will correspond to the environment-specific observations for each genotype, while DL^{s} (predictor variable) could either be based on the BVP for the same particular genotype or a common reference representing all genotypes. The choice depends first on whether BVP data are available for all genotypes in the MET, but also whether different genotypes in the same environment experience large or small differences in photoperiod.

Statistical analysis of the PRN-FTP

Two different regression functions, bilinear and linear, were used for modeling the PRN-FTP. This involved two different approaches as follows:

Bilinear function for estimating three parameters of the PRN-FTP. With a sufficient density of data and coverage of DL^{s} spanning SD and LD environments, photoperiod sensitive genotypes are expected to follow a bilinear pattern of response. In SD environments $T_{\mathrm{t}}^{\mathrm{em-ant}}$ remains constant, and above a critical threshold for LD environments it increases linearly with photoperiod. For this, the PRN-FTP can be modeled as a continuous two-phase (bilinear) regression function with threshold detection (Fong *et al.*, 2017*a*). We used the "hinge model" in the R package *chngpt* (Fong *et al.*, 2017*b*), defined as follows:

$$T_{\mathrm{t}}^{\mathrm{em-ant}} = \alpha + \beta(DL^{s} - e)_{+} \qquad \text{(Eq. 2)}$$

where $T_{\mathrm{t}}^{\mathrm{em-ant}}$ (described before) is the response variable; e is the threshold parameter; DL^{s} is the sensed daylength with a threshold effect; $I(DL^{s} > e) = 1$ when $DL^{s} > e$ and 0 if $DL^{s} \leq e$; $(DL^{s} - e)_{+}$ denotes the hinge function, which equals $DL^{s} - e$ for $DL^{s} > e$ and 0 otherwise; and α and β are the intercept and slope parameters, respectively. The model was fitted using default settings for *chngpt*, with no constraints set for estimating the threshold value (breaking point of the bilinear model). Estimated effects include an intercept, threshold value, and slope, which correspond to physiological components of flowering time: flowering time *per se*, a critical threshold for photoperiod sensitivity, and photoperiod sensitivity, respectively.

Linear function for estimating two parameters of the PRN-FTP. When fitting the bilinear model is not feasible due to insufficient density of data, inadequate coverage of DL^{s} for threshold detection, or because it is not an appropriate model for all genotypes (i.e., photoperiod insensitive genotypes), we modeled the PRN-FTP as a linear regression function, forgoing threshold estimation. So that the intercept for $T_{\mathrm{t}}^{\mathrm{em-ant}}$ is estimated at the mean DL^{s} of SD environments rather than the shortest day environment, environments across the MET were first classified as SD or LD based on whether DL^{s} falls below or above a fixed threshold, respectively (we used 13.5 h which corresponded to the average threshold estimated from the analysis of Dataset D4, see results). The predictor values for each environment were then recoded as the mean DL^{s} value for the respective SD and LD environments in the regression model. Finally, when specifying the linear regression model, the SD and LD DL^{s} means are offset with the mean SD-DL^{s} value set to zero to obtain the proper intercept estimate for the corresponding genotype. Hereafter, we refer to this as the "LD-SD" method for modeling the PRN-FTP. This is similar to prior studies that used the difference between mean thermal times to flowering in LD and SD environments as an estimate of photoperiod senstivity (Coles *et al.*, 2010; Hung *et al.*, 2012), except here an intercept for flowering time *per se* (in units °C) and slope for photoperiod sensitivity (in units °Ch^{-1}) are estimated.

N.B.—Two particular points are relevant for interpreting parameters estimated by the LD-SD method. First, envirotyping of DL^{s} to obtain the mean values for SD and LD environments may be based on each specific genotype being modeled or a common reference genotype (this point is described in other parts of the study). Even if a common reference BVP is used to envirotype DL^{s} for all genotypes, the mean values for DL^{s} can vary due to imbalanced observations of the genotypes across environments, which occurs frequently in MET data. That is, although DL^{s} may be envirotyped for a common reference BVP in each environment, the regression analysis is performed using predictor values linked to the observed $T_{\mathrm{t}}^{\mathrm{em-ant}}$ data being modeled for each genotype. Second, for photoperiod sensitive genotypes, it is expected that estimates of photoperiod sensitivity will be biased as a function of the deviation between the SD-DL^{s} value and the true (unknown) critical photoperiod for a given genotype. When the true critical photoperiod is less than the SD-DL^{s} value, the estimate will be upward biased, and when it is greater it will be downward biased.swart

Correction for latent variables affecting thermal times to anthesis. If only temperature influenced the flowering time of a photoperiod insensitive genotype, we expect its $T_{\mathrm{t}}^{\mathrm{em-ant}}$ would be nearly identical across all environments in an MET. However, aside from photoperiod sensitivity, misrepresentation in the temperature response function, or measurement error, deviations in $T_{\mathrm{t}}^{\mathrm{em-ant}}$ could be due to various possibilities that vary from one environment to another, including the influence of other environmental factors, differences in crop management practices, differences between air temperature and the temperature sensed by the crop, imprecision and biases in weather data, or other latent variables. Therefore, with dataset D4, we tested an alternative approach using photoperiod insensitive control

genotypes to adjust for the effects of latent variables across environments prior to constructing the PRN-FTP.

Seven photoperiod insensitive genotypes were defined as control genotypes in Dataset D4. The 37 environments comprising the MET were assembled from different experiments. Unfortunately, all seven control genotypes were not present in all environments, so two sets of control groups were defined (set 1: B37, B73, M37W, Mo17, and Oh43; set 2: LH123Ht and 2369). Sets 1 and 2 were associated with 22 and 15 of the environments, respectively. For each set, the overall mean of $T_{\mathrm{t}}^{\mathrm{em-ant}}$ was calculated across environments of the MET in which they were present. The environment-specific residuals were then used to adjust the thermal times for the remaining non-control genotypes in each corresponding environment. We note that using two sets of control genotypes that were also imbalanced across environments (see the earlier description of Dataset D4) is not ideal and could introduce some bias, but any improvement in the model fit would presumably reflect positively on this approach. Therefore, using Dataset D4, we compared the overall RMSE of the PRN-FTP model fit and standard errors of parameter estimates before and after applying the correction method.

Applications of the PRN-FTP

Datasets D4 and D5 were used to test the concepts developed in this study for modeling and analyzing the PRN-FTP from MET data.

Methodological evaluation. The MET for Dataset D4 had a sufficient coverage of DL^s for fitting the bilinear model (assumed to be the biologically correct one). Additionally, BVP values from Dataset D2 could be used to obtain genotype-specific DL^s values for the genotypes in D4. This allowed us to test different approaches to modeling the PRN-FTP, including: (i) the impact of using latent-variable adjusted values of $T_{\mathrm{t}}^{\mathrm{em-ant}}$; (ii) the impact of envirotyping DL^s using genotype-specific values versus a common reference value for the BVP; and (iii) the impact of using the bilinear model versus the LD-SD method on the estimated parameters for flowering time *per se* and photoperiod sensitivity (the threshold for critical photoperiod can only be estimated with the bilinear model). Although this was performed with only seven tropical maize genotypes, analysis with the bilinear model also provided a preliminary survey of potential variation in the three PRN-FTP parameters for maize.

Analysis of maize diversity. We sought to investigate the wider variation in PRN-FTP parameters in a diverse collection of 214 maize genotypes adapted to different geographical zones (Dataset D5). However, due to both an insufficient density and coverage of DL^s and the mixed composition of photoperiod sensitive and insensitive genotypes, the bilinear function could not be fit. This was true even for genotypes known to be photoperiod sensitive, such as those used for methodological evaluation (we observed bogus estimates of the parameters). Moreover, most of the genotypes were not present in Dataset D2 so genotype-specific BVP values for DL^s envirotyping could not be systematically used. Therefore, for Dataset D5, the LD-SD method was applied, with DL^s values obtained using the BVP for the 50th-percentile reference maturity determined with Dataset D2 (Table 1). The regression model was fit using latent-variable adjusted BLUEs for $T_{\mathrm{t}}^{\mathrm{em-ant}}$ regressed onto mean DL^s for the SD and LD environments as described in the previous section. Latent variable adjustment was performed using the set 1 control group (indicated above) common across the Dataset D5 MET.

Results

Choosing a temperature response function to construct the PRN-FTP

Thermal time is used to determine DL^s for envirotyping along with T_t^{em-ant} for modeling the PRN-FTP, such that different temperature response functions for calculating thermal time could result in different outcomes. A comparison of three different temperature response functions showed no significant difference in the NRMSEs for thermal times to anthesis for 24 photoperiod-insensitive hybrids tested in 25 to 26 environments in North America. Regardless of the temperature response function that was tested, for each hybrid, the environment-specific thermal time to anthesis deviated, on average, by ~10% (range 9 to 13%) from the across-environment mean (Fig. S1). Therefore, for the current study, we chose the non-linear response function by Wang and Engel (1998) adapted for maize (Eq. S2) due to its common implementation in crop growth models (Wang *et al.*, 2017), its higher physiological realism compared with the linear response function (Eq. S1), and its greater flexibility compared to the Arhenus model (Parent *et al.*, 2010).

Predicting when maize becomes sensitized to photoperiod

There is no known visible marker to measure the timing when maize plants become sensitized to photoperiod for determining DL^s. Therefore, we defined this using the BVP (T_t^{em-TI} in SD conditions), which closely corresponds to the thermal time required for plants to reach their photoperiod-sensitized stage (Kiniry *et al.*, 1983*b*; Bassiri *et al.*, 1992). An issue is that directly observing tassel initiation requires temporal dissections of shoot apical meristems which is not possible at a large scale. To circumvent this, we used an ecophysiological formalism to estimate T_t^{em-TI} (Eq. 1) for the 284 genotypes in panel A grown under SD conditions (Dataset D2; File S2). A separate SD experiment validated this for eight of the genotypes using microscopy data on differentiation of shoot apical meristems into tassel primordia (Methods S2). The Pearson correlation coefficient between predicted and observed BVP values was 0.84, indicating the formalism-based predictions for T_t^{em-TI} align closely with observational data. Table 1 summarizes percentiles of the BVP distribution for panel A, with the 5th, 50th, and 95th percentile values used to represent early, medium, and late maturity groups for envirotyping DL^s.

Spatiotemporal variation in the sensed photoperiod for maize

Envirotyping with DL^s can be used to understand how different genotypes sense photoperiod across and within environments, and how this varies according to spatiotemporal patterns in climate and weather. To examine how photoperiods are perceived by maize, we computationally envirotyped DL^s for 671 field environments across the Northern Hemisphere where maize has been previously grown (Fig. 2).

We first summarized the spatial axis of variation in DL^s using the 50th percentile of T_t^{em-TI} (326 °Cd) as a common reference for envirotyping (Table 1; Fig. S2). The range in DL^s across the entire set of environments evaluated was 11.9 to 18.3 h, a difference of 6.4 hours (Fig. 2a). We compared the DL^s for maize above 30° N in the USA and Europe, corresponding to regions where maize is used extensively for scientific research and agricultural production (Figure 2a-b). Mean DL^s across the USA was 16.1 h and in Europe was 16.7 h, with lower (5-percentile) to upper (95-percentile) ranges of 14.3 to 16.4 and 15.7 to 17.5, respectively. These spatial patterns are primarily driven by climatic variation in photoperiod across latitude coupled with the seasonality for maize cultivation. Since temperature can speed or slow growth and development, interannual differences in temperature and planting dates at the same location can give rise to additional variation in DL^s for maize. To examine this, we selected 118 field sites where maize was planted for at least two years and found that DL^s within a single location varied by as much as 1.7 hours, with a mean absolute difference of 0.3 h.

Next, we questioned the extent to which multiple genotypes grown within the same field environment perceive a different photoperiod. Beyond the equator, photoperiod is not constant across days of the year, with increasing rates of daily change in association with latitude. Therefore, genotypes differing in BVP that reach their photoperiod-sensitized stage on different days would perceive a different photoperiod (Fig. 2b-c), but to our knowledge the magnitude by which this varies has not been investigated. Using the 5th (239 °Cd) and 95th (434 °Cd) percentiles of the BVP distribution (Table 1) to represent early and late percentile-maturity groups, the DL^s at these limits frequently differed by more than 1 h, with the largest difference reaching 3.8 h (Fig. 2b). Differences in DL^s above 2 h were rare and occurred only in locations at high latitudes where late genotypes are not cultivated for maize production. Nevertheless, this highlights how the genetic diversity of maize can intersect with environmental variation within the same field, leading to differences in the photoperiod to which genotypes respond.

If the 50th-percentile for BVP is used as a common reference for envirotyping DL^s, the magnitude of inaccuracy compared to genotype-specific DL^s varies according to the specific set of genotypes used and the environment in which they are tested. For instance, the early and late percentile-maturity groups differed from the 50th-percentile reference by as little as no difference to as much as 1.4 h and 2.4 h, respectively (File S3). The larger differences occurred at higher latitudes where daily rates of photoperiodic change were greatest. As expected, this difference reduced to zero as a function of decreasing rates in photoperiodic change (Fig. 2d).

Using METs for modeling the PRN-FTP

To test approaches for modeling the PRN-FTP from METs, we combined flowering time data from multiple projects totaling 37 field experiments (Dataset D4) that included, albeit with imbalanced data (Table S1), a common set of seven genotypes of tropical origin that were expected to be photoperiod sensitive. This was used to compare procedures for estimating genotype-specific PRN-FTP parameters for flowering time *per se* (intercept), critical photoperiod (threshold), and photoperiod sensitivity (slope) using a two-phase regression model (see Methods; Fig. 3).

Using MET data to construct the PRN-FTP makes the simplistic assumption that physiological sensitivities to temperature and photoperiod are the only environmental factors influencing flowering time. Although these are dominant factors, other variables can also affect maize growth and development, but the specific causes are often unknown and likely to vary from one field environment to another. Therefore, we devised an approach to control for latent effects on flowering time and evaluated how adjusted values for the $T_{\mathrm{t}}^{\mathrm{em-ant}}$-phenotypic axis affected PRN-FTP parameter estimation. Using a designated set of photoperiod-insensitive control genotypes present in the D4 MET, their overall mean $T_{\mathrm{t}}^{\mathrm{em-ant}}$ across environments was defined as an expected value for the specific effect of temperature on flowering time (i.e., for photoperiod insensitive genotypes, $T_{\mathrm{t}}^{\mathrm{em-ant}}$ is expected to be the same across environments, with deviations attributed to latent variables; see Materials and Methods). Then, environment-specific deviations from the overall mean were used to adjust the $T_{\mathrm{t}}^{\mathrm{em-ant}}$ values for the remaining genotypes in each of the corresponding environments. Fig. 3 portrays this procedure and how it can affect estimates of the PRN-FTP parameters.

When tested using genotype-specific DL^s values for each of the seven tropical genotypes, latent variable adjustment of $T_{\mathrm{t}}^{\mathrm{em-ant}}$ enhanced the precision of the overall model fit of the PRN-FTP by an average of two-fold (Table 2). Using adjusted values also led to changes in the estimated thresholds of sensitivity, which in turn resulted in differences in the estimated flowering times *per se* by as much as 5% and slopes of sensitivity by as much as 77% (Table 2).

As described in the previous section, genotypes with a different BVP can experience different photoperiods within environments, such that points along the DL^s-environmental axis of the PRN-FTP may differ among genotypes in a common MET. This caused us to question the standard approach to modeling reaction norms from METs where all genotypes are assumed to experience the same environmental conditions in each field (i.e., values for a given environmental covariate is assumed to be common for all genotypes). If the specific conditions experienced by different genotypes are sufficiently large, this could impact parameter estimates of a reaction norm. To test this, we compared modeling the PRN-FTP using DL^s obtained from the BVP for each genotype versus the 50th-percentile BVP as a common reference. The seven genotypes presented adequate variation for testing this: compared to the 50th-percentile reference point, genotype-specific values for the BVP ranged from 266 ºCd to 399 ºCd, corresponding to the 16th and 89th percentiles of the BVP distribution estimated from 284 genotypes (Table 1). However, the set of environments in the MET network of Dataset D4 presented smaller contrasts in DL^s than would occur at higher latitude (European) environments (Fig. 2b): the largest difference in DL^s between these specific genotypes and the common reference was 0.22 h. In this case, changes in coefficient estimates for thresholds of sensitivity and flowering time *per se* were negligible, but the slope parameter for photoperiod sensitivity changed by 12% for one of the gentoypes (Table 2). Nevertheless, these results show that intra-environment variation in DL^s among genotypes can affect PRN-FTP parameters estimated from MET data. Even for this small sample of genotypes, Fig. 4 highlights a wide range of diversity for flowering time plasticity in maize consisting of unique parameterizations of the PRN-FTP.

Relating components of the PRN-FTP to understand maize adaptation

Since flowering time *per se* and photoperiod sensitivity underlie flowering time adaptation across environments (Choquette *et al.*, 2023), we questioned how the trait space of these PRN-FTP parameters is structured among primary breeding pools of maize. For this, we assembled an MET dataset (D5) from 19 field trials with a common set of genotypes consisting of tropical, temperate, and admixed breeding material. Computational envirotyping showed that DL^s for the D5 MET was restricted to two small intervals of photoperiod conditions, with three environments of 11.9 to 12.4 h photoperiod and 16 environments of 14.5 to 16.5 h photoperiod. With this density of data and gap in coverage of DL^s, the bilinear function for the PRN-FTP could not be reliably fit. Besides, the collection of material included photoperiod insensitive genotypes that do not follow a bilinear response to photoperiod. In this case, the PRN-FTP was modeled using an LD-SD method based on linear regression after, as previously described, adjusting for latent variables with a designated set of control genotypes. Examining the relationship between flowering time *per se* and photoperiod sensitivity showed that temperate and tropical material occupy distinct territories of the trait space (Fig. 5; File S6). Temperate genotypes tend to have a lower flowering time *per se* and nearly no photoperiod sensitivity, while tropical genotypes tend to have a higher flowering time *per se* coupled with a large range in photoperiod sensitivity. Fitting genetic expectations for polygenic traits, genotypes with admixed ancestry are positioned between these two regions of the trait space.

Discussion

Understanding trait plasticity is important for adapting crops to new environments. To study the variation in plastic responses, METs allow large collections of genotypes to be characterized across environmental gradients. When modeling genotype-environment effects, the assumption—implicit in standard models—is that all genotypes experience the same conditions in each environment (an exception: (Millet *et al.*, 2019)). However, as demonstrated in this study, due to phenological variation and stage-specific sensitivities, different genotypes within each field environment may not experience

523 identical environmental conditions. This can complicate the definition of environmental indices for
524 modeling reaction norms from METs, challenging standard analyses that assume common
525 environmental conditions are sensed by all genotypes. Based on the ecophysiology of maize flowering
526 time, the current study defines a new metric, DL^s, for quantifying the specific photoperiods sensed by
527 different genotypes within and across environments. Using DL^s to envirotype maize fields in the
528 Northern Hemisphere, we showed that, at high latitudes, where cooler temperatures that slow
529 development combine with relatively large daily rates of photoperiodic change, genotypes in the same
530 environment can experience more than a 1 h difference in DL^s (Fig. 2). This occurs more often and is
531 more pronounced across maize environments in Europe than in the U.S. due to higher rates of daily
532 photoperiodic change (Fig. 2d). Thus, to provide more accurate information about the variation in trait
533 plasticity, the construction of genotype-specific reaction norms for flowering time and other traits
534 should be considered on a case-by-case basis.

535 Constructing the PRN-FTP from METs is the most practical approach for studying the diversity of
536 flowering time plasticity, but this is challenged by the geographical structure of photoperiod (Fig. 2)
537 and the sensitivity of parameter estimation to gaps in DL^s (Table 2, Fig. 4). Testing across numerous
538 field sites spanning nearly an entire hemisphere is required to capture a sufficient range and density of
539 DL^s to model genotypic variation in the PRN-FTP. We found that currently available MET datasets for
540 maize do span LD and SD conditions but have limited to no coverage of DL^s from 12.4 to 14.5 h, the
541 specific range for expected variation in the critical photoperiod for maize (Rood and Major, 1980;
542 Kiniry *et al.*, 1983*a*). With scant information on critical photoperiods for maize, and given the
543 dependence of accurate threshold estimation for regression analysis of the PRN-FTP (Table 2),
544 envirotyping with DL^s could be used to design new METs for future research on flowering time
545 plasticity.

546 The PRN-FTP provides a parsimonious model for flowering time plasticity, taking into account the
547 dominant effects of temperature and photoperiod. However, in METs, latent variables can affect
548 flowering time, requiring appropriate adjustments. In particular, constructing the PRN-FTP from
549 thermal time estimates can be obscured by the influence of other factors besides temperature on growth
550 and development, such as drought (e.g., Harrison *et al*., 2014; Herrero and Johnson 1981). To address
551 this issue, we applied a between-environment covariate adjustment using photoperiod-insensitive
552 control genotypes expected to have the same thermal time to anthesis across LD and SD environments.
553 This consistently resulted in a more precise fit of the bilinear response function for the PRN-FTP (Table
554 2; Fig. 3). Nevertheless, it is important to acknowledge that the choice of a control group could
555 introduce some bias, as it may uniquely vary in other ecophysiological responses. Another challenge
556 in modeling the PRN-FTP is that not all genotypes exhibit a clear bilinear response. For example,
557 photoperiod-insensitive genotypes only display differences in flowering time *per se*, rendering the
558 bilinear regression function invalid. In such cases, linear regression using the LD-SD method is the
559 most appropriate way of capturing the relationship between $T_{\mathrm{t}}^{\mathrm{em-ant}}$ and DL^s. Thus, while the PRN-
560 FTP offers a valuable framework for understanding flowering time plasticity, careful consideration of
561 latent effects, choice of control group, and genotype-specific responses is necessary for accurate
562 modeling. Future work could consider alternative statistics to simultaneously model mixtures of
563 genotypes with bilinear and linear reaction norm structures for the PRN-FTP.

564 A large body of work has elucidated the GRN-topology of multiple pathways involved in the
565 transduction of signals that control flowering time in plants (Srikanth and Schmid, 2011). Reflective
566 of this complex regulatory system, MET mapping studies have shown the genetic architecture of
567 phenotypic variation in days to flowering to be polygenic (e.g., maize - Buckler et al., 2009). While

568 many genes are involved, using ecophysiology to redefine the context for genetic mapping can clarify
569 the roles of individual loci or genes in relation to the GRN. As one example from maize, mapping
570 variation in the difference between thermal time to flowering in LD and SD environments—an
571 ecophysiological transformation of days to flowering into a measure of photoperiod sensitivity—led
572 to the identification of a causal variant affecting the regulation of the photoperiod sensitivity pathway
573 (Hung *et al.*, 2012; Yang *et al.*, 2013). The same study by Hung *et al*. (2013) demonstrated that this
574 approach isolates loci specifically responsive to photoperiod from other loci that contribute to variation
575 in flowering time in other ways. Nevertheless, the full topology and context-dependent expression of
576 the GRN regulating flowering time remains unresolved, let alone its connections across physiological
577 to whole-plant scales. We expect that using DL^s-guided MET design to estimate and decompose
578 variation in flowering time *per se*, critical photoperiods, and photoperiod sensitivity will help to further
579 disentangle the genetic architectures of these context-specific traits. By relating these architectures to
580 the GRN, this approach will facilitate testing of hypotheses on the multiscalar relationships and
581 genotype-environnment interactions for flowering time.

582 Flowering time adaptations have facilitated the evolution and geographical spread of plant species
583 (Gaudinier and Blackman, 2019). The expansion of maize from its tropical origins to shorter growing
584 seasons in the temperate zone was mediated by selection for early flowering time (Vigouroux *et al.*,
585 2008; Tenaillon and Charcosset, 2011; Swarts *et al.*, 2017), with evidence of selection on multiple
586 pathways of the GRN (Brandenburg *et al.*, 2017). Distinct breeding material was established from
587 locally preadapted populations that have largely persisted as separate pools of tropical and temperate
588 maize (Liu *et al.*, 2003). Taken together, we reasoned that the PRN-FTP trait space of flowering time
589 *per se* and photoperiod sensitivity for modern varieties representing these pools would reflect the
590 historical perspective of adaptation and subsequent breeding in maize. Figure 5 corroborates this:
591 assuming tropical genotypes reflect an ancestral state defined by moderate to late flowering time *per*
592 *se* (adaptation to long growing seasons in the tropics) and segregation for photoperiod sensitivity (weak
593 to no selection in SD environments), temperate maize shows both reduced flowering time *per se* and
594 photoperiod sensitivity (adaptations for a shortened crop cycle). While this general structuring of
595 plasticity between tropical and temperate breeding pools could be expected, Fig. 5 reveals an empty
596 territory of the space where essentially no genotypes exist that are both early *per se* and strongly
597 sensitive to photoperiod. This combination could also condition moderate maturity, for example. We
598 hypothesize that this is a byproduct of the preadaptation history and subsequent breeding of maize, and
599 not indicative of an intrinsic coupling between different pathways of the GRN or physiological controls
600 of flowering time. This is supported by results from experimental evolution for early flowering time in
601 tropical populations under contrasting photoperiod conditions. In LD environments, photoperiod
602 sensitivity and flowering time *per se* are co-selected but show different rates change across generations,
603 with photoperiod sensitivity rapidly eliminated (Teixeira *et al.*, 2015; Choquette *et al.*, 2023). In
604 contrast, in SD environments, responses to selection can be attributed to flowering time *per se* with no
605 changes observed for photoperiod sensitivity. This highlights how the PRN-FTP can be used for
606 studying crop diversity, and that knowledge about the historical context of adaptation and breeding can
607 aid in interpreting the observed patterns in the PRN-FTP-derived trait space.

608 **Conclusions**

609 In this study, we explored various aspects of a physiological reaction norm for modeling flowering
610 time plasticity in maize. Envirotyping with DL^s is a valuable tool for examining the global distribution
611 of photoperiodic sensing in maize and constructing the PRN-FTP from MET data. Notably, the
612 geographical distribution of current public MET networks for maize are concentrated in LD and SD
613 environments with discontinuity in DL^s across the critical photoperiod range. This hinders investigation

of the PRN-FTP for maize and accurate modeling of flowering time $G \times E$, warranting further experimentation. The DL^s index can be used for the design of new MET networks to address this.

The PRN-FTP model provides an ecophysiological framework for decomposing and understanding phenotypic variation in flowering time measured in days. For a specific genotype, the pace of development towards reproductive transition is affected by temperature fluctuations within an environment, with the magnitude of this influence varying across environments based on the unique temperature patterns. When contrasting genotypes are present in the same environments, interactions between temperatures and genetic variation in rates of development (phyllochron) and durations of reproductive transition (BVP) gives rise to variation in the timing of photoperiod sensitization. In turn, genetic variation in critical thresholds and photoperiod sensitivities lead to secondary interactions with daily rates of photoperiodic change and exposure to further temperature fluctuations within and across environments. This highlights the interplay between genetic and environment effects that shape phenotypic variation in flowering time.

Lastly, as the PRN-FTP model is based on common ecophysiological processes, we expect that it can be extended to other crops. Investigating the trait space of PRN-FTP components could provide valuable insights into flowering time adaptations across species. Our findings underscore the significance of considering the historical context of adaptation and breeding in unraveling the genetic and physiological underpinnings of complex traits. This, in turn, holds promising implications for future crop improvement endeavors.

Acknowledgements: This study was made possible thanks to the production and availability of datasets from prior and ongoing projects: the EXPOSE and PhotoGrid projects at INRAE-LEPSE (ANR-16-IDEX-0006; France 2030 program; Post AgreenSkills Fund), the INVITE project (European Union's Horizon 2020 research and innovation program, grant no. 817970), the Maize ATLAS project (USDA-ARS, grant no. 2011-67003-30342), the Multiple Disease Resistance project (North Carolina State University, Cornell University, and University of Delaware collaboration), the Genomes-to-Fields Initiative (https://www.genomes2fields.org/home/), and the Panzea project (NSF-PGRP, grant no. 1238014). We wish to thank a number of people who contributed to this study: (i) Mainassara Abdou Zaman-Allah, Terence Molnar, and Prasanna Boddupalli from CIMMYT for providing much of the germplasm used for panel A; (ii) Alexis Bédiée, Llorenç Cabrera-Bosquet, Nicole Choquette, Arnaud Desbiez-Piat, Thomas Laisné, Noé Lalouette-Marrier d'Unienville, Maëlle Lis, Anthony Rosello, Javier Soto Mendoza, and Benoît Suard for supporting the PhenoArch platform experiments at Montpellier, FR; (iii) Arnaud Brunet, Bernard Lagardere, and Jean-Rene Loustalot from the experimental station at Saint-Martin-de-Hinx, FR for supporting germplasm management and field testing; (iv) the ISRA team Ibrahima Sarr, Malick Ndiaye, Awa Mbengue, Abdoulaye Hoth, and Alain Audebert (CIRAD) for field trial data from Nioro du Rip, SN; and (v) the Moreno Retis team José Moreno and Luis Rodríguez for field trial data from Puerto Vallarta, MX.

Author Contributions:

JD, RJW: conceptualization; CP, CW, RJW: resources; JD, CP, KJ, EM, RJW: investigation; JD, CP, JR, RJW: data curation; JD, PM, BP, RJW: methodology; JD, JR, KJ, RJW: formal analysis; JD, RJW: writing - original draft; EM, JR, PM, KJ: writing - review & editing; BP, CW, RJW: supervision; EM, RJW: funding acquisition.

Conflict of Interest: The authors declare that the research was conducted in the absence of any commercial or financial relationships that could be construed as a potential conflict of interest.

Funding Statement: This work was supported by the French National Research Agency (ANR-16-IDEX-0006 and ANR-24-CE45-3875-01), the France 2030 program, project EXPOSE (PAF_18) supported by INRAE, and the European Union's Horizon 2020 research and innovation program, grant no. 817970.

Data Availability: Data and metadata from this study are available in Supplementary Files at Dryad (https://doi.org/10.5061/dryad.x95x69pth). Sources of data are indicated in the methods sections and Table S1 (also see acknowledgments). Computer code for envirotyping DL^s and fitting the PRN-FTP is available at: https://github.com/maizeatlas/prnftp.

References

Andrieu B, Hillier J, Birch C. 2006. Onset of sheath extension and duration of lamina extension are major determinants of the response of maize lamina length to plant density. Annals of Botany **98**, 1005–1016.

Bassiri A, Irish EE, Poethig RS. 1992. Heterochronic effects of Teopod 2 on the growth and photosensitivity of the maize shoot. Plant Cell **4**, 497–504.

Bendix C, Mendoza JM, Stanley DN, Meeley R, Harmon FG. 2013. The circadian clock-associated gene gigantea1 affects maize developmental transitions. Plant, Cell and Environment **36**, 1379–1390.

Blümel M, Dally N, Jung C. 2015. Flowering time regulation in crops-what did we learn from Arabidopsis? Current Opinion in Biotechnology **32**, 121–129.

Bonhomme R, Derieux M, Kiniry JR, Edmeades GO, Ozier-Lafontaine H. 1991. Maize leaf number sensitivity in relation to photoperiod in multilocation field trials. Agronomy Journal **83**, 153–157.

Bonnett OT. 1954. The inflorescences of maize. Science **120**, 77–87.

Bradshaw AD. 1965. Evolutionary significance of phenotypic plasticity in plants. phenotypic plasticity **23**, 207–215.

Brandenburg JT, Mary-Huard T, Rigaill G, Hearne SJ, Corti H, Joets J, Vitte C, Charcosset A, Nicolas SD, Tenaillon MI. 2017. Independent introductions and admixtures have contributed to adaptation of European maize and its American counterparts. PLoS Genetics **13**, 1–30.

Buckler ES, Holland JB, Bradbury PJ, *et al.* 2009. The genetic architecture of maize flowering time. Science **325**, 714–718.

Buckley LB, Briones Ortiz BA, Caruso I, John A, Levy O, Meyer A V., Riddell EA, Sakairi Y, Simonis JL. 2023. TrenchR: An R package for modular and accessible microclimate and biophysical ecology. PLOS Climate **2**, e0000139.

Cabrera-Bosquet L, Fournier C, Brichet N, Welcker C, Suard B, Tardieu F. 2016. High-throughput estimation of incident light, light interception and radiation-use efficiency of thousands of plants in a phenotyping platform. New Phytologist **212**, 269–281.

Choquette NE, Holland JB, Weldekidan T, Drouault J, de Leon N, Flint-Garcia S, Lauter N, Murray SC, Xu W, Wisser RJ. 2023. Environment-specific selection alters flowering-time plasticity and results in pervasive pleiotropic responses in maize. New Phytologist **238**, 737–749.

Colasanti J, Coneva V. 2009. Mechanisms of floral induction in grasses: Something borrowed, something new. Plant Physiology **149**, 56–62.

Coles ND, McMullen MD, Balint-Kurti PJ, Pratt RC, Holland JB. 2010. Genetic control of photoperiod sensitivity in maize revealed by joint multiple population analysis. Genetics **184**, 799–812.

Cooper M, Tang T, Gho C, Hart T, Hammer G, Messina C. 2020. Integrating genetic gain and gap analysis to predict improvements in crop productivity. Crop Science **60**, 582–604.

Dong Z, Danilevskaya O, Abadie T, Messina C, Coles N, Cooper M. 2012. A gene regulatory network model for Floral transition of the shoot apex in maize and its dynamic modeling. PLoS ONE **7**.

Ducrocq S, Madur D, Veyrieras JB, Camus-Kulandaivelu L, Kloiber-Maitz M, Presterl T,

Ouzunova M, Manicacci D, Charcosset A. 2008. Key impact of *Vgt1* on flowering time adaptation in maize: Evidence from association mapping and ecogeographical information. Genetics **178**, 2433–2437.

Finlay KW, Wilkinson GN. 1963. The analysis of adaptation in a plant-breeding programme. Australian Journal of Agricultural Research **14**, 742–754.

Flint-Garcia SA, Thuillet AC, Yu J, Pressoir G, Romero SM, Mitchell SE, Doebley J, Kresovich S, Goodman MM, Buckler ES. 2005. Maize association population: A high-resolution platform for quantitative trait locus dissection. Plant Journal **44**, 1054–1064.

Fong Y, Chongzhi D, Huang Y, Gilbert PB. 2017*a*. Model-robust inference for continuous threshold regression models. Biometrics **73**, 452–462.

Fong Y, Huang Y, Gilbert PB, Permar SR. 2017*b*. chngpt: Threshold regression model estimation and inference. BMC Bioinformatics **18**, 1–7.

Forsythe WC, Rykiel EJ, Stahl RS, Wu H i., Schoolfield RM. 1995. A model comparison for daylength as a function of latitude and day of year. Ecological Modelling **80**, 87–95.

Gaudinier A, Blackman BK. 2019. Evolutionary processes from the perspective of flowering time diversity. New Phytologist **225**, 1883–1898.

Guo L, Wang X, Zhao M, *et al.* 2018. Stepwise cis-regulatory changes in *ZCN8* contribute to maize flowering-time adaptation. Current Biology **28**, 3005-3015.e4.

Guo T, Wei J, Li X, Yu J. 2023. Environmental context of phenotypic plasticity in flowering time in sorghum and rice. Journal of Experimental Botany **75**, 1004–1015.

Harrison MT, Tardieu F, Dong Z, Messina CD, Hammer GL. 2014. Characterizing drought stress and trait influence on maize yield under current and future conditions. Global Change Biology **20**, 867–878.

Herrero MP, Johnson RR. 1981. Drought Stress and Its Effects on Maize Reproductive Systems. Crop Science **21**, 105–110.

Hung HY, Shannon LM, Tian F, *et al.* 2012. *ZmCCT* and the genetic basis of day-length adaptation underlying the postdomestication spread of maize. Proceedings of the National Academy of Sciences **109**, E1913–E1921.

Itoh H, Nonoue Y, Yano M, Izawa T. 2010. A pair of floral regulators sets critical day length for Hd3a florigen expression in rice. Nature Genetics **42**, 635–638.

Jarquín D, Crossa J, Lacaze X, *et al.* 2014. A reaction norm model for genomic selection using high-dimensional genomic and environmental data. Theoretical and Applied Genetics **127**, 595–607.

Kiniry JR. 1991. Maize Phasic Development. In Modeling Plant and Soil Systems (eds J. Hanks and J.T. Ritchie). https://doi.org/10.2134/agronmonogr31.c4.

Kiniry JR, Ritchie JT, Musser RL. 1983*a*. Dynamic nature of the photoperiod response in maize. **10**, 10–13.

Kiniry JR, Ritchie JT, Musser RL, Flint EP, Iwig WC. 1983*b*. The photoperiod sensitive interval in maize. Agronomy Journal **75**, 687–690.

Kusmec A, Srinivasan S, Nettleton D, Schnable PS. 2017. Distinct genetic architectures for phenotype means and plasticities in *Zea mays*. Nature Plants **3**, 715–723.

Lee SH, Choi CW, Park KM, *et al.* 2021. Diversification in functions and expressions of soybean *FLOWERING LOCUS T* genes fine-tunes seasonal flowering. Frontiers in Plant Science **12**, 1–16.

Lejeune P, Bernier G. 1996. Effect of environment on the early steps of ear initiation in maize (*Zea mays* L.). Plant, Cell and Environment **19**, 217–224.

Liu K, Goodman M, Muse S, Smith JS, Buckler E, Doebley J. 2003. Genetic structure and diversity among maize inbred lines as inferred from DNA microsatellites. Genetics **165**, 2117–2128.

Matsubara K, Yamanouchi U, Wang ZX, Minobe Y, Izawa T, Yano M. 2008. *Ehd2*, a rice ortholog of the maize Indeterminate1 gene, promotes flowering by up-regulating Ehd1. Plant Physiology **148**, 1425–1435.

McFarland BA, Alkhalifah N, Bohn M, *et al.* 2020. Maize genomes to fields (G2F): 2014-2017 field seasons: Genotype, phenotype, climatic, soil, and inbred ear image datasets. BMC Research Notes **13**, 4–9.

Meng X, Muszynski MG, Danilevskaya ON. 2011. The *FT*-like *ZCN8* gene functions as a floral activator and is involved in photoperiod sensitivity in maize. Plant Cell **23**, 942–960.

Millet EJ, Kruijer W, Coupel-Ledru A, Alvarez Prado S, Cabrera-Bosquet L, Lacube S, Charcosset A, Welcker C, van Eeuwijk F, Tardieu F. 2019. Genomic prediction of maize yield across European environmental conditions. Nature Genetics **51**, 952–956.

Minow MAA, Ávila LM, Turner K, Ponzoni E, Mascheretti I, Dussault FM, Lukens L, Rossi V, Colasanti J. 2018. Distinct gene networks modulate floral induction of autonomous maize and photoperiod-dependent teosinte. Journal of Experimental Botany **69**, 2937–2952.

Muller B, Martre P. 2019. Plant and crop simulation models: Powerful tools to link physiology, genetics, and phenomics. Journal of Experimental Botany **70**, 2339–2344.

Nemoto Y, Nonoue Y, Yano M, Izawa T. 2016. *Hd1*, a *CONSTANS* ortholog in rice, functions as an *Ehd1* repressor through interaction with monocot-specific CCT-domain protein Ghd7. The Plant Journal **86**, 221–233.

Padilla JM, Otegui ME. 2005. Co-ordination between leaf initiation and leaf appearance in field-grown maize (*Zea mays*): Genotypic differences in response of rates to temperature. Annals of Botany **96**, 997–1007.

Parent B, Tardieu F. 2012. Temperature responses of developmental processes have not been affected by breeding in different ecological areas for 17 crop species. New Phytologist **194**, 760–774.

Parent B, Turc O, Gibon Y, Stitt M, Tardieu F. 2010. Modelling temperature-compensated physiological rates, based on the co-ordination of responses to temperature of developmental processes. Journal of Experimental Botany **61**, 2057–2069.

Park SJ, Kim SL, Lee S, *et al.* 2008. Rice Indeterminate 1 (*OsId1*) is necessary for the expression of *Ehd1* (Early heading date 1) regardless of photoperiod. Plant Journal **56**, 1018–1029.

Rising J, Devineni N. 2020. Crop switching reduces agricultural losses from climate change in the United States by half under RCP 8.5. Nature Communications **11**, 1–7.

Rogers AR, Dunne JC, Romay C, *et al.* 2021. The importance of dominance and genotype-by-environment interactions on grain yield variation in a large-scale public cooperative maize experiment. G3: Genes, Genomes, Genetics **11**.

Rood SB, Major DJ. 1980. Responses of early corn inbreds to photoperiod. Crop Science **20**, 679–682.

Roof DA. 1997. *Evolutionary quantitative genetics*.

Sawa M, Kay SA. 2011. GIGANTEA directly activates *Flowering Locus T* in *Arabidopsis thaliana*.

Proceedings of the National Academy of Sciences **108**, 11698–11703.

Sawa M, usinow, Dmitri A., Steve KA, Imaizumi T. 2007. FKF1 and GIGANTEA complex formation is required for day-length measurement in *Arabidopsis*. Science **318**, 261–265.

Simpson GG, Dean C. 2002. *Arabidopsis*, the Rosetta stone of flowering time? Science **296**, 285–289.

Sloat LL, Davis SJ, Gerber JS, Moore FC, Ray DK, West PC, Mueller ND. 2020. Climate adaptation by crop migration. Nature Communications **11**, 1–9.

Song YH, Shim JS, Kinmonth-Schultz HA, Imaizumi T. 2015. Photoperiodic flowering: Time measurement mechanisms in leaves. Annual Review of Plant Biology **66**, 441–464.

Sparks A. 2018. nasapower: A NASA POWER global meteorology, surface solar energy and climatology data client for R. Journal of Open Source Software **3**, 1035.

Srikanth A, Schmid M. 2011. Regulation of flowering time: All roads lead to Rome. Cellular and Molecular Life Sciences **68**, 2013–2037.

Stephenson E, Estrada S, Meng X, Ourada J, Muszynski MG, Habben JE, Danilevskaya ON. 2019. Over-expression of the photoperiod response regulator *ZmCCT10* modifies plant architecture, flowering time and inflorescence morphology in maize. PLoS ONE **14**, 1–32.

Swarts K, Gutaker RM, Benz B, *et al.* 2017. Genomic estimation of complex traits reveals ancient maize adaptation to temperate North America. Science **357**, 512–515.

Teixeira JEC, Weldekidan T, De Leon N, *et al.* 2015. Hallauer's Tusón: A decade of selection for tropical-to-temperate phenological adaptation in maize. Heredity **114**, 229–240.

Tenaillon MI, Charcosset A. 2011. A European perspective on maize history. Comptes Rendus - Biologies **334**, 221–228.

Vigouroux Y, Glaubitz JC, Matsuoka Y, Goodman MM, Sánchez G. J, Doebley J. 2008. Population structure and genetic diversity of New World maize races assessed by DNA microsatellites. American Journal of Botany **95**, 1240–1253.

van Voorn GAK, Boer MP, Truong SH, Friedenberg NA, Gugushvili S, McCormick R, Bustos Korts D, Messina CD, van Eeuwijk FA. 2023. A conceptual framework for the dynamic modeling of time-resolved phenotypes for sets of genotype-environment-management combinations: a model library. Frontiers in Plant Science **14**, 1–14.

Wang E, Engel T. 1998. Simulation of phenological development of wheat crops. Agricultural Systems **58**, 1–24.

Wang E, Martre P, Zhao Z, *et al.* 2017. The uncertainty of crop yield projections is reduced by improved temperature response functions. Nature Plants **3**, 1–11.

Yang Q, Li Z, Li W, *et al.* 2013. CACTA-like transposable element in *ZmCCT* attenuated photoperiod sensitivity and accelerated the postdomestication spread of maize. Proceedings of the National Academy of Sciences **110**, 16969–16974.

Zabel F, Müller C, Elliott J, *et al.* 2021. Large potential for crop production adaptation depends on available future varieties. Global Change Biology **27**, 3870–3882.

Zhao Y, Zhao B, Xie Y, *et al.* 2023. The evening complex promotes maize flowering and adaptation to temperate regions. Plant Cell **35**, 369–389.

833 **List of Tables and Figures**

834 **Table 1.** Percentiles of the distribution for the basic vegetative phase (BVP) in panel A.

835 **Table 2.** Impact of latent variable adjustment and genotype-specific envirotyping on PRN-FTP
836 parameter estimation for different maize genotypes.

837 **Figure 1.** Graphical guide to the study.

838 **Figure 2.** Envirotyping of sensed photoperiod across and within maize fields in the Northern
839 Hemisphere.

840 **Figure 3.** Adjusting for latent variable effects across a multi-environment trial network when fitting
841 the PRN-FTP.

842 **Figure 4.** The PRN-FTP for seven tropical genotypes of maize.

843 **Figure 5.** The trait space for flowering time *per se* and photoperiod sensitivity in maize breeding
844 material.

845 **Table 1. Percentiles of the distribution for the basic vegetative phase (BVP) in panel A.**

	Min	5%	25%	50%	75%	95%	Max
BVP (ºCd)	169	239	286	326	375	434	496

846

847 **Table 2. Impact of latent variable adjustment and genotype-specific envirotyping on PRN-FTP**
848 **parameter estimation for different maize genotypes.**

Genotype	Intercept (ºCd)	Threshold (h)	Slope (ºCd h^{-1})	RMSE[a]
Unadjusted values with genotype-specific *DL*^{s}				
CML10	851.0 ± 28.6	12.3 ± 0.6	44.3 ± 9.7	82.0
CML258	934.6 ± 33.4	12.3 ± 0.7	42.1 ± 11.4	95.4
CML277	856.5 ± 22.1	14.5 ± 0.6	96.7 ± 18.7	76.0
CML341	802.0 ± 24.7	12.3 ± 0.6	49.1 ± 8.4	71.2
CML373	815.2 ± 30.6	12.3 ± 1.1	35.9 ± 10.7	67.5
Tzi8	858.0 ± 29.1	12.4 ± 1.1	30.9 ± 9.9	86.4
Tzi9	809.0 ± 29.5	12.2 ± 1.1	26.3 ± 9.3	85.0
Adjusted values with genotype-specific *DL*^{s}				
CML10	872.8 ± 16.7	12.3 ± 0.6	36.9 ± 5.6	47.7
CML258	953.8 ± 21.2	12.3 ± 0.9	37.7 ± 7.2	60.5
CML277	869.8 ± 9.2	14.5 ± 0.6	87.7 ± 8.0	31.3
CML341	846.0 ± 9.8	14.3 ± 0.6	86.7 ± 7.9	33.8
CML373	853.1 ± 11.6	12.3 ± 0.8	26.4 ± 4.0	25.6
Tzi8	888.8 ± 14.7	14.3 ± 1.0	44.3 ± 10.7	52.8
Tzi9	842.1 ± 11.2	14.4 ± 0.9	41.8 ± 8.8	40.0
Adjusted values with common reference *DL*^{s}				
CML10	873.7 ± 16.5	12.3 ± 0.6	37.5 ± 5.7	47.6
CML258	955.8 ± 21.0	12.3 ± 0.9	37.7 ± 7.3	60.5
CML277	870.2 ± 9.3	14.3 ± 0.5	77.0 ± 7.1	32.1
CML341	846.9 ± 9.9	14.3 ± 0.6	83.2 ± 7.6	34.2
CML373	853.5 ± 11.5	12.2 ± 0.8	26.3 ± 4.0	25.5
Tzi8	888.6 ± 14.7	14.5 ± 1.1	47.9 ± 11.6	52.8
Tzi9	841.9 ± 11.2	14.5 ± 0.8	43.2 ± 9.0	39.9

849 [a]Root mean squared error (RMSE) is reported for the full bilinear model.

Figure 1. Graphical guide to the study.

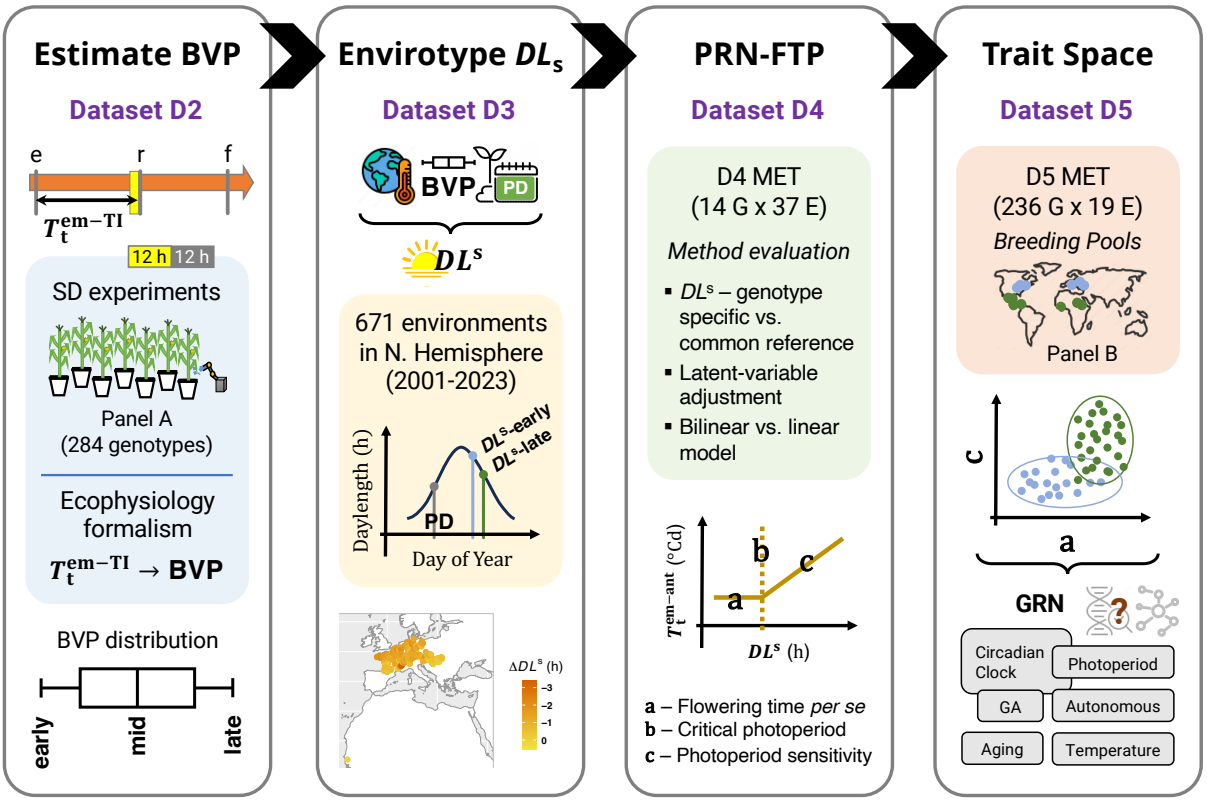

Each panel portrays the main parts of the study performed with Datasets 2-4 (Dataset 1 was used to evaluate the choice of a temperature response function for calculating thermal time, not shown): (i) The estimation of basic vegetative phase (BVP) follows from prior research showing that the photoperiod-sensitized stage is reached just prior to the thermal-time required for reproductive transition (T_t^{em-TI}) plants grown under SD conditions. This is depicted by the filled arow marked with the timing of emergence ("e"), reproductive transition ("r"), and flowering ("f"). The orange shading of the arrow represents that plants sense temperature throughout their life cycle, while the yellow box represents that photoperiod begins to be sensed at a particular time. Data from short-day (SD) experiments were used to estimate the BVP distribution for 284 genotypes in panel A. (ii) The temperature data from maize fields, BVP reference values for early, mid, and late maturing genotypes, and planting dates ("PD") were used to envirotype the daylength sensed (DL^s) by each maturity class in 671 environments. The figure in the shaded region depicts how DL^s can vary between early and late maturing genotypes that become sensitized to photperiod on different days of the year (this can vary due to fluctuations in temperature and rates if photoperiodic change). This was used to characterize inter- and intra-environmental variation in DL^s for maize in the Northern Hemisphere. (iii) The physiological reaction norm for flowering time plasticity (PRN-FTP) was modeled using MET data on 14 genotypes in 37 environments. An evaluation of the methodologies for modeling the PRN-FTP was performed as noted in the shaded area. The figure portrays the PRN-FTP modeled as a bilinear function with coefficient estimates for flowering time *per se* (a, units °C), critical photoperiod (b, units: h), and photoperiod sensitivity (c, units: °Ch^{-1}). (iv) The PRN-FTP was

872 modeled as a linear function (LD-SD method, see text) using MET data on 214 genotypes (panel B)
873 in 19 environments. The trait space defined by flowering time *per se* (a) and photoperiod sensitivity
874 (c) was used to infer about historical adaptation in maize. The map in the shaded area portrays
875 genotypes from temperate (blue) and tropical (green) breeding pools of maize comprising panel B.
876 The trait-space plot reflects a finding of this study, showing that tropical and temperate breeds
877 occupy different territories of the space. Future research on the genetic dissection of the separate
878 parameters may be used to relate ecophysiological scale variation to pathways in the gene regulator
879 network (GRN) for reproductive transition and flowering time.

880

Figure 2. Envirotyping of sensed photoperiod across and within maize fields in the Northern Hemisphere.

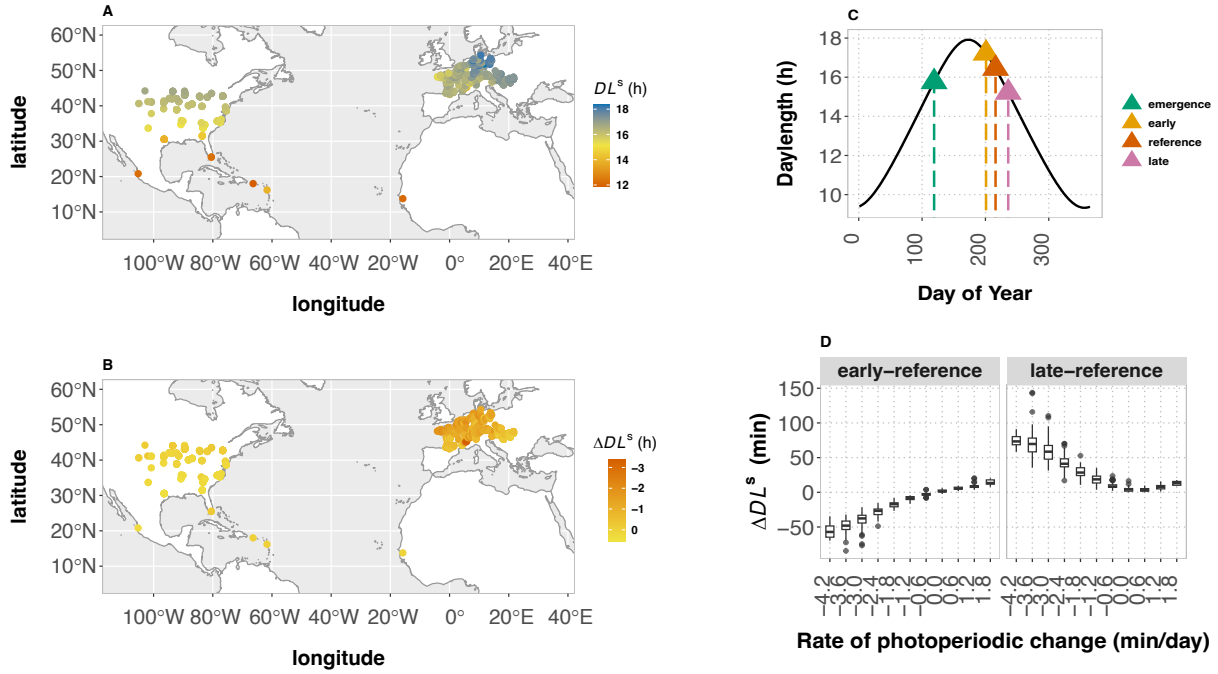

(A) Sensed photoperiod (DL^s for the 50th-percentile maturity reference) across maize field sites in the Northern Hemisphere. (B) Within environment differences in hours of sensed daylength (ΔDL^s) between the 95th and 5th percentile maturity groups defined by the BVP distribution of panel A. (C) The figure portrays how different maturity groups can reach the photoperiod sensitized stage on different days of the year within the same environment, leading to differences in DL^s (the 5th, 50th, and 95th percentile values of the BVP in panel A are indicated as early, reference, and late maturity groups) (D) The relationship between within environment differences in DL^s and rates of daily photoperiodic change. Here, the differences are shown in minutes for comparisons between the reference maturity group relative to the early and late maturity groups. As reflected in (B), the boxplots show that genotypes within the same environment experience increasingly greater differences in photoperiods when rates of photoperiodic change increase, which occurs in association with increasing latitude.

Figure 3. Adjusting for latent variable effects across a multi-environment trial network when fitting the PRN-FTP.

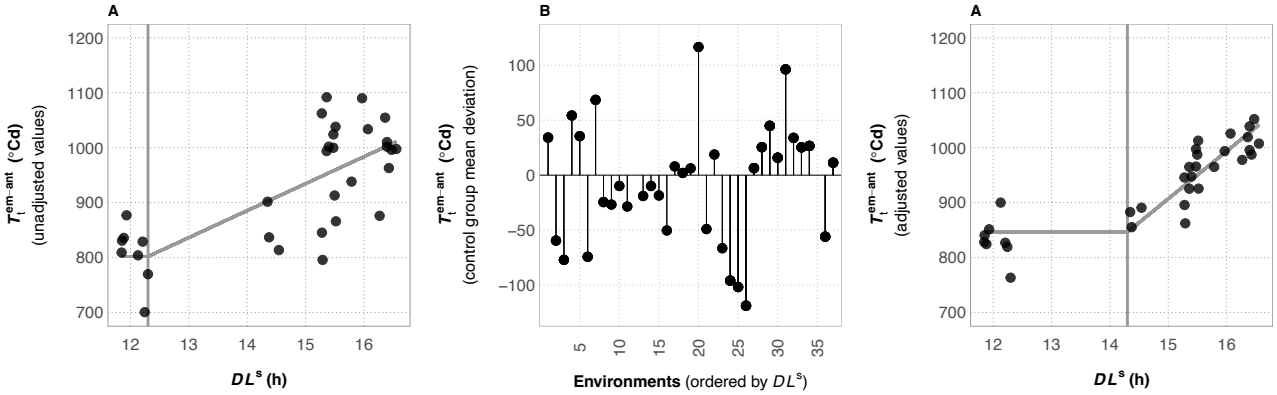

(A) The plot shows the PRN-FTP for genotype CML341, using unadjusted BLUEs for thermal time from crop emergence to anthesis (T_t^{em-ant}; black points). The grey lines show the estimated flowering time *per se* (horizontal line), critical threshold value (vertical line), and photoperiod sensitivity (sloped line). (B) Deviations from the overall average T_t^{em-ant} for the control groups of photoperiod insensitive genotypes estimated across the same environments, with the environment identifiers ordered as in plots (A) and (B) according to sensed daylength (DL^s). (C) The PRN-FTP for genotype CML341 after adjusting the BLUEs by deviations in (B), leading to different estimates for the flowering time *per se*, the critical threshold value, and the photoperiod sensitivity.

907 **Figure 4. The PRN-FTP for seven tropical genotypes of maize.**

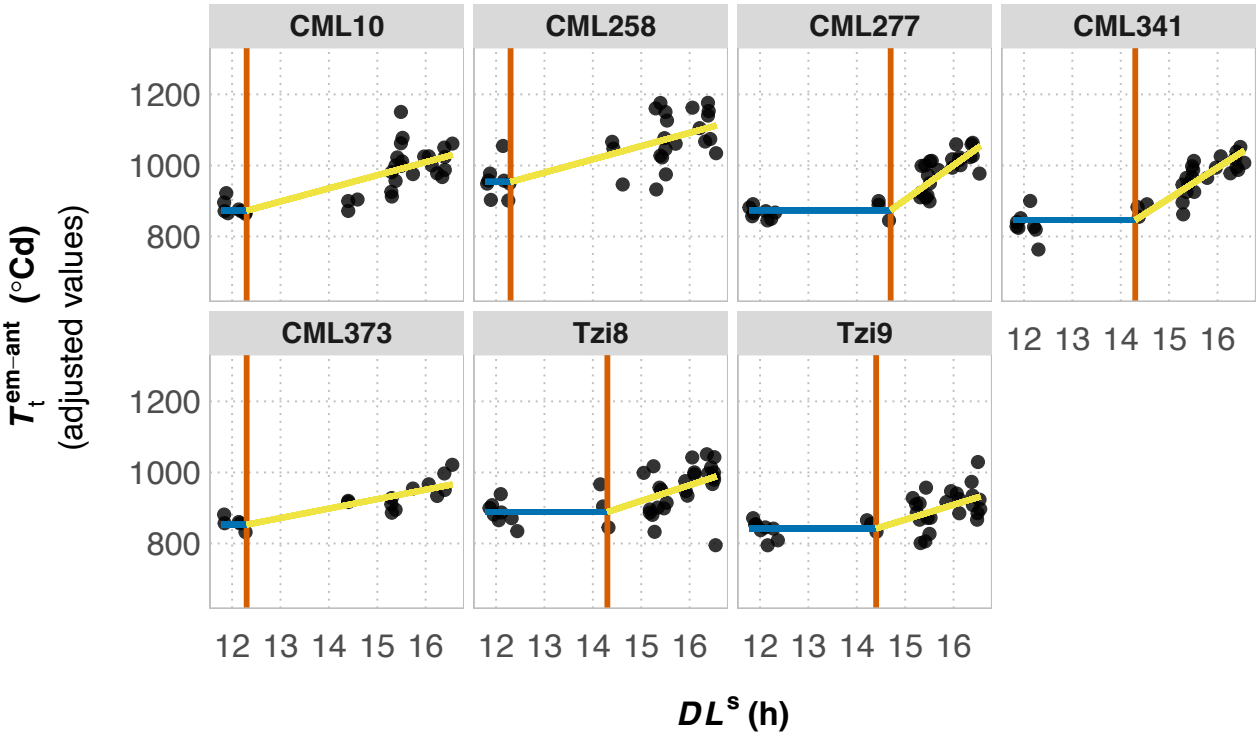

908

909 (A) For each genotype, the plots show the three PRN-FTP parameters estimated from the bilinear
910 function fitted using latent-variable adjusted BLUEs for thermal time from crop emergence to anthesis
911 (T_t^{em-ant}) in relation to sensed daylength (DL^s). Parameter estimates are shown for the flowering time
912 *per se* (blue line), the critical threshold value (red line), and the photoperiod sensitivity (yellow line).

913 **Figure 5. The trait space for flowering time *per se* and photoperiod sensitivity in maize breeding**
914 **material.**

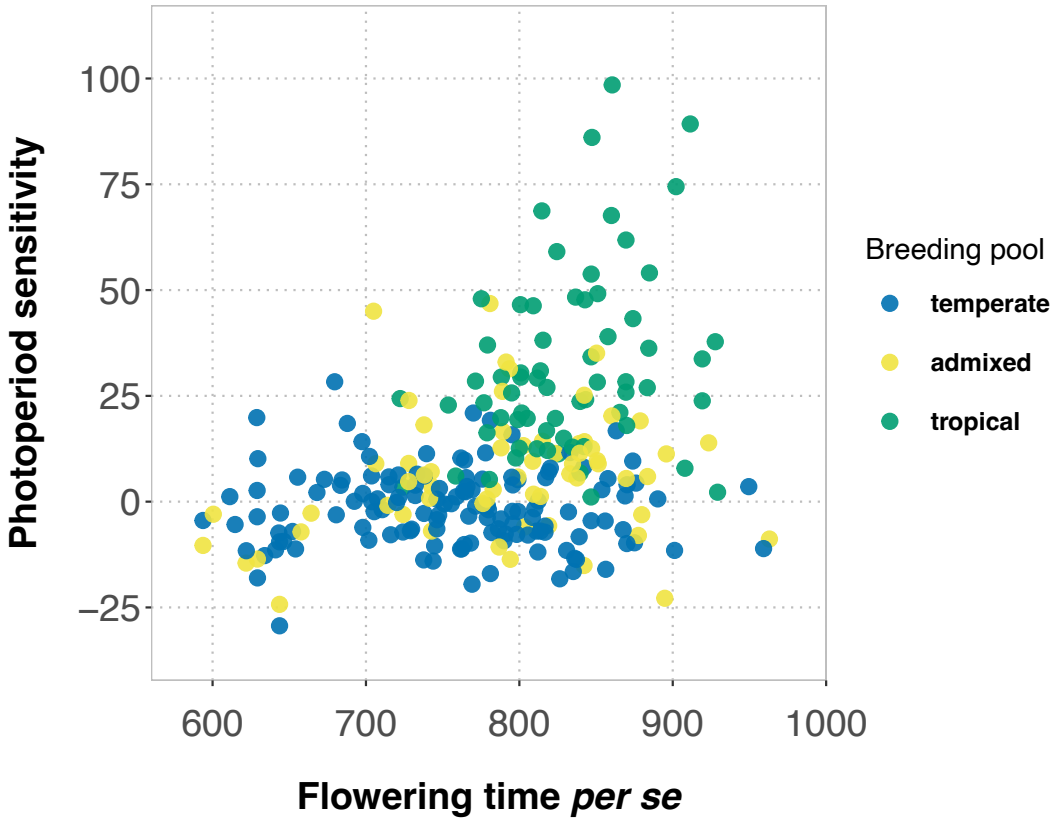

915

916 Points correspond to genotypic values for flowering time *per se* (ºCd) and photoperiod sensitivity
917 (ºCd h^{-1}), estimated using the LD-SD regression method on latent-variable adjusted BLUEs.
918 Breeding pools are represented by genotypes previously assigned to temperate (*n*=137), admixed
919 (*n*=62), and tropical (*n*=66) sources based on structure analysis of marker data (Flint-Garcia *et al.*,
920 2005).